Performance of the Pressure Assisted Forward Osmosis-MSF Hybrid Desalination Plant

Daoud Khanafer[1], Sudesh Yadav[1], Namuun Ganbat[1], Ali Altaee[1]*, John Zhou[1], Alaa Hawari[2]

[1]Centre for Green Technology, School of Civil and Environmental Engineering, University of Technology Sydney, 15 Broadway, NSW, 2007, Australia
[2]Department of Civil and Architectural Engineering, Qatar University, P.O. Box 2713, Doha, Qatar.
*Corresponding author email address: ali.altaee@uts.edu.au, tel: +61-295149668

Abstract

Osmotically driven membrane process was proposed for seawater pretreatment to multi-stage flashing (MSF) thermal plant. Brine reject from the MSF plant was the draw solution (DS) in the FO process in order to reduce chemical use. The purpose of forward osmosis (FO) is the removal of divalent ions from seawater prior the thermal desalination. In this study, seawater at 80 g/L and 45 g/L concentrations was used as the brine reject and seawater, respectively. The temperature of the brine reject was 40°C and of seawater was 25°C. Commercial thin-film composite (TFC) and cellulose triacetate (CTA) membranes were evaluated for the pretreatment of seawater in the FO and the pressure-assisted FO (PAFO) processes. Experimental results showed 50% more permeation flux by increasing the feed pressure from 1 to 4 bar, and permeation flux reached 16.7 L/m²h in the PAFO process with a TFC membrane compared to 8.3 L/m²h in the PAFO process with CTA membrane. TFC membrane experienced up to 15% reduction in permeation flux after cleaning with DI water while permeation flux reduction in the CTA membrane was > 6%. The maximum recovery rate was 11.5% and 8.8% in the PAFO process with TFC and CTA membrane, respectively. The maximum power consumption for the pretreatment of seawater was 0.06 kWh/m³ and 0.1 kWh/m³ for the PAFO process with a TFC and CTA membrane, respectively.

1. Introduction

Seawater desalination has become a strategic source of clean water worldwide and specifically in the area of the Middle East, where the natural resources are limited (Intelligence et al., 2011; Yadav et al., 2020). Reverse Osmosis (RO) represents the primary membrane technologies for desalination, while thermal technologies are mainly the Multi-Stage Flushing (MSF) and to a less extent, the Multi-Effect Distillation (MED) (Al-Karaghouli and Kazmerski, 2013; Gilron, 2014). Thermal desalination is responsible for 70% of the total freshwater supply in the Middle East due to their high performance for treatment treating feed solutions of high salinity and low quality, reliability, and no need for intensive pretreatment of feed solution (Mabrouk, 2013). Despite the advantages of thermal desalination processes, they suffer from scale formation on the heat exchangers due to the precipitation of alkaline such as calcium carbonate ($CaCO_3$) and non-alkaline such as calcium sulfate ($CaSO_4$) and magnesium sulfate ($MgSO_4$) scaling. Scale precipitation adversely impacts the performance of thermal desalination plants and the energy requirements for desalination (El Din et al., 2002; Hassan, 2006). Periodic cleaning and antiscalants are often applied to minimize scaling problems, however, cannot prevent it (Mabrouk, 2013), particularly non-alkaline scale in the MSF plants, which requires shutting down the MSF plant for cleaning (Lyster et al., 2010). Recently, Forward Osmosis (FO) was suggested for the pretreatment of seawater to the MSF plants for the removal of multivalent ions, causing scale problems in heat exchangers. When coupling the FO with the MSF plant, the MSF brine concentrate will be used as the draw solution (DS) to reduce the operation cost (Altaee et al., 2014). The feed water in the FO membrane is seawater that would be pretreated for the removal of divalent ions (**Figure 1**). The purpose of the FO process is to dilute the concentration of divalent ions in the brine reject before recycling to the MSF unit to minimize/prevent the precipitation of magnesium sulfate and calcium sulfate on the surface of heat exchangers. Previous research revealed the viability of applying the FO process in minimizing scale problems and increasing the top brine temperature (TBT) in the MSF plant (Altaee et al., 2014; Thabit et al., 2019). It is noticeable that research on the FO technology

for the treatment of seawater to MSF/MED systems is scarce, and more work is required to understand the role of membrane materials and applied feed pressure on the FO process. Driven by the osmotic pressure gradient across the membrane, FO was introduced as a pretreatment process in the cycle of the MSF desalination plant (Altaee et al., 2014). The innovation in the model proposed is that the brine rejected from the MSF plants plays the role of DS and the seawater is the feed solution (FS) in the membrane. The outcome is promising in minimizing the concentration of multivalent ions in the feed water to the MSF plant. The diluted brine will return to the MSF system as a lower salinity FS with the potential to reduce scale deposition and allows the MSF plant to work at elevated TBT (Altaee et al., 2014). Moreover, the proposed FO-MSF system might solve the issue of hot brine rejection of the sea and reduce the seawater intake (Altaee et al., 2014). The FO-MSF system was theoretically designed, and its feasibility has investigated to reveal a potential reduction in Ca^{2+}, Mg^{2+} and SO_4^{2-} ions concentrations.
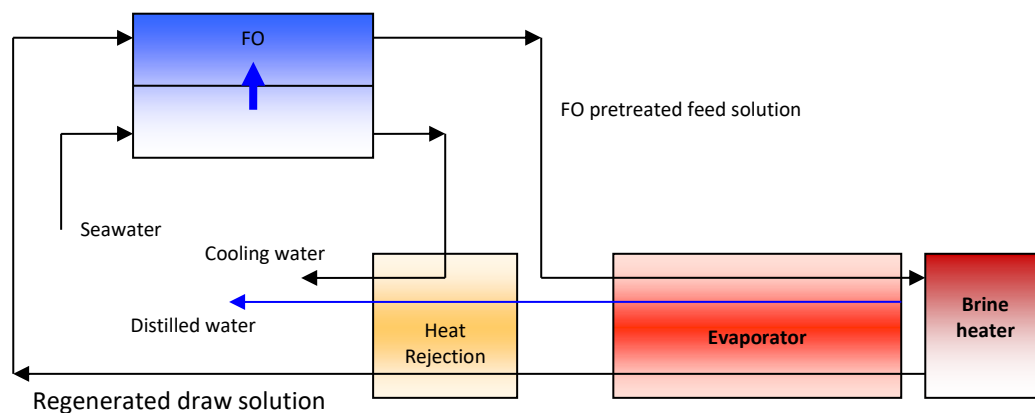

Figure 1: FO pretreatment of seawater to the MSF plant.

Although theoretical studies underpinned the potential of FO-MSF system, there were only a few experimental studies in this field. Thabit et al. (Thabit et al., 2019) studied the efficiency of the FO technology for seawater treatment using cellulose triacetate FTSH_2O membrane and actual brine reject DS at 40ºC. The FO membrane tested in the PRO mode [DS-AL (Active Layer)] achieved 22.3 L/m²h permeation flux exceeded and 8.5% dilution of the DS brine at the end of the experiment. The outcomes of the study formed a foundation that needs building upon with more experiments to deeper investigate and evaluate the adoption of FO-

MSF system in the Middle East. Type of membrane materials and operating modes also affects membrane fouling propensity and permeation flux. To understand the impact of membrane materials, researchers investigated the impact of membrane materials on the efficiency of the FO process (Chung et al., 2012; Mazlan et al., 2016; Yadav et al., 2020). Livingston et al., studied fouling in cellulose triacetate (CTA) and Thin-film composite (TFC) membranes (Mazlan et al., 2016). They found that membrane surface roughness dominated over fouling layer properties when the active layer is against the FS or in the AL-FS mode. In another study investigating the efficiency of the FO technology in CTA and TFC membranes, it revealed that permeation flux in the TFC was greater than that in the CTA membrane (Chung et al., 2012). Previous studies also examined the impact of operating parameters on the efficiency of the FO process. A study by Alaa et al. (Hawari et al., 2016) evaluated the impact of the temperatures of feed and draw solution's on the FO process revealed that permeation flux could be increased when the temperature of the draw solution increased from 20 to 26°C. Increasing DS temperature over 26°C resulted in a gradual decline in permeation flux due to the phenomenon of thermos-osmosis. Permeation flux in the FO technology is mainly driven by the osmotic pressure gradients across the membrane. However, several studies tested pressure-assisted FO (PAFO) to improve the permeation flux and tackling the influence of concentration polarization in the membrane (Blandin et al., 2013; Oh et al., 2014). The concept of PAFO consists of applying a small feed pressure to increase the permeation flow under the effect of both osmotic and hydraulic pressures (Coday et al., 2013) for the reason that the AL-FS mode is known for causing severe dilutive internal concentration polarization (ICP). A study by Jamil and co-workers evaluated the feasibility of PAFO for the treatment of RO brine and results showed 2% and 29% increase in the permeation flux by applying 2 and 4 bar, respectively (Jamil et al., 2016). The latter outcome encouraged a similar path of research and development in FO technology using the concept of PAFO.

The current study evaluated the performance of PAFO process in the pretreatment of seawater to the MSF plant. Instead of using a pressure-driven nanofiltration membrane for seawater softening, the FO process is applied as a pretreatment for the dilution of brine reject due to its energy efficiency (Van der Bruggen and Luis, 2015). A seawater brine of 80 g/L concentration and 40°C was the DS in the FO membrane to resemble the concentration and temperature of the MSF brine reject in the Middle East. The FS in the FO membrane was seawater of 45 g/L concentration, and 25°C that represent the conditions of seawater in the

Middle East. Also, there is no information available yet on the influence of membrane materials on the performance of the FO-MSF system, knowing that both TFC and CTA FO membranes are commercially available. Porifera TFC and FTSH_2O CTA membranes were tested to find out the influence of membrane materials on the efficiency of the FO process and permeation flux recovery after membrane cleaning. The TFC and CTA membrane was tested in the FO and PAFO modes using 0 to 4 bar feed pressure since previous studies showed discrepancies in the process efficiency when it operates under different membrane orientations. The permeation flow, rejection rate to Ca^{2+}, Mg^{2+} and SO_4^{2-} ions, and the process recovery rate were calculated in the FO and the PAFO modes for TFC and CTA membranes. Reduction in the permeation flux due to membrane fouling was evaluated for both membranes and under different operational modes to determine the most efficient type of membrane and operating mode for the FO-MSF system. The study also estimated the specific power consumption for the CTA and the TFC membrane to evaluate the impact of the type of membrane and its operating mode on the power consumption of the FO process.

2. Methodology

2.1 FO membranes and characterization

Porifera TFC and FTSH_2O CTA membranes were implemented in this study to test their performance under different operating parameters. As shown in **table 1** and referring to the manufacturer guideline, the thin-film composite membrane from Porifera has a structural parameter (*S*) of 344 microns. The membrane can tolerate pressure up to 12.41 bar, 40°C feed temperature and salt rejection capability up to 90% (Blandin et al., 2016). Similarly, the datasheet from FTSH_2O summarised the characteristics of the cellulose triacetate membrane presented in **table 1** (Madsen et al., 2017). This membrane can tolerate up to 50°C feed temperature and hydraulic pressure of 5 bar.

Table 1: Characteristics of Porifera and FTSH_2O membranes.

Parameter	Porifera (TFC)	FTSH_2O (CTA)
Membrane chemistry	Thin-film composite	Cellulose triacetate
A (L/m²h.bar)	2.1	0.69
B (L/m²h)	1.2	0.34
S (μm)	344	707
Contact angle active layer	68.5°±0.7	68.1° ± 1
Contact angle support layer	53.9° ± 2	60.2° ± .5
Zeta potential	-41.9 ± 2.44	-12.8 ± 1.18

In **table 1**, A represents the water permeability constant, B represents the coefficient of solute permeability, and S is the membrane structural parameter. A was calculated using the following expression:

$$A_w = \frac{J_w}{\Delta P} \qquad (1)$$

Where J_w is the water flux in L/m²h and ΔP is the pressure gradient across the membrane in bar. In its turn, B was also calculated using the following expression:

$$B = \frac{(1-R_j)}{R_j} J_w \qquad (2)$$

Where R_j is the rejection rate of the membrane and J_w is the water flux. The Values of A and B presented in this paper were also reported in previous studies (Madsen et al., 2017). Wettability measurements and hydrophilic behaviour of the virgin Porifera TFC and FTSH_2O CTA membranes were investigated by measuring the contact angle using the sessile drop method at various places on the same membrane, and it is measured using FACE Automatic Interfacial Tensiometer (Japan). Images of water contact angle measurement are represented in **Figure 2**. Surface morphology of the used and cleaned membranes for AL-DS direction was obtained using a scanning electron microscope (SEM, Zeiss Supra 55VP). All the membranes were washed with deionized (DI) water and subsequently dried in a vacuum chamber before characterization. Zeta potential measurements were carried out for virgin Porifera TFC and FTSH_2O CTA membranes using Malvern instruments. The wettability of membranes measures

the wetting angle between the interface of the surface of the water and the outline of the membrane surface. The active layer (AL) of Porifera TFC and FTSH$_2$O CTA membrane shows almost an equal water contact angle ~ 68.5 and 68.1, respectively, (**Figure 2**). As for the support layer, Porifera TFC showed lower water contact angle, ~ 53.9, than FTSH$_2$O CTA membrane, ~60.2.
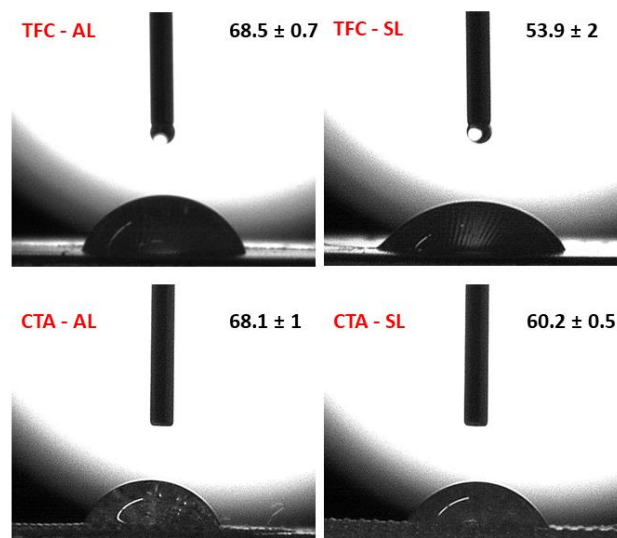

Figure 2: Water contact angle for virgin Porifera TFC and FTSH$_2$O CTA membranes.

2.2 Feed and Draw solutions

In this study, fresh seawater was collected from the Sydney area with a salinity of 32g/L and concentrated by heating to increase its concentration to the level of brine reject and seawater from the MSF plants. In all experiments, the concentration of the FS was 45g/L and of the DS was 80 g/L. Also, the temperature of FS was 25°C and of the DS was 40°C to resemble the temperature of brine reject (Thabit et al., 2019). As a primary step, seawater was stored in containers and left for at least two days for the large particles to settle. **Table 2** shows the compositions and characteristics of the FS and the DS used in the experimental work.

Table 2: Characteristics of FS and DS.

Ion / parameter	FS (45g/L)	DS (80g/L)	Measuring Instrument
Ca^{2+}(ppm)	855.2	1040.9	7900 ICP-MS
Mg^{2+}(ppm)	1895.3	2199.6	7900 ICP-MS
SO_4^{2-}(ppm)	3171.6	6566	DIONEX AS-AP
Cl^-(ppm)	9832	22351.6	7900 ICP-MS
Na^+(ppm)	16372.9	19151.6	7900 ICP-MS
K^+(ppm)	692.9	872.3	7900 ICP-MS
TDS (g/L)	45.1	80.2	HQ14d Conductivity
Conductivity (mS/cm)	68.9	106.7	HQ14d Conductivity
pH	8.0	8.35	HQ40d multi
Turbidity (NTU)	1.47	2.43	2100P Turbidimeter

2.3 FO system components

FO membranes were placed in the CF042A-FO Cell manufactured by Sterlitech. This clear cast acrylic cube-shaped cell is a filtration unit of 5×4×3,25-inch exterior dimensions and includes 42 cm^2(6.5 inch^2) membrane area. The cell can tolerate 88°C maximum temperature and 27.6 bar of hydraulic pressure. The system was provided with 2 flow meters F-550 (Blue-White Industries Ltd) connected on each side of the cell to measure the flow rates of the FS and DS. The system is furnished with pressure gauges (USG U.S. Gauge) with a range between 0 and 4 bar to measure the hydraulic pressure on the FS and DS. Water circulation in the system was maintained by using two pumps manufactured by Cole-Parmer providing up to 5 bar. The conductivity of solutions, as well as the TDS and the salinity, were measured using HQ 14d portable conductivity and TDS meter (HACH, Australia). The variation in the FS weight was monitored using a digital scale balance and forwarded to a computerized system to calculate the permeation flux. **Figure 3** shows an illustration of the FO unit used in the experimental work.
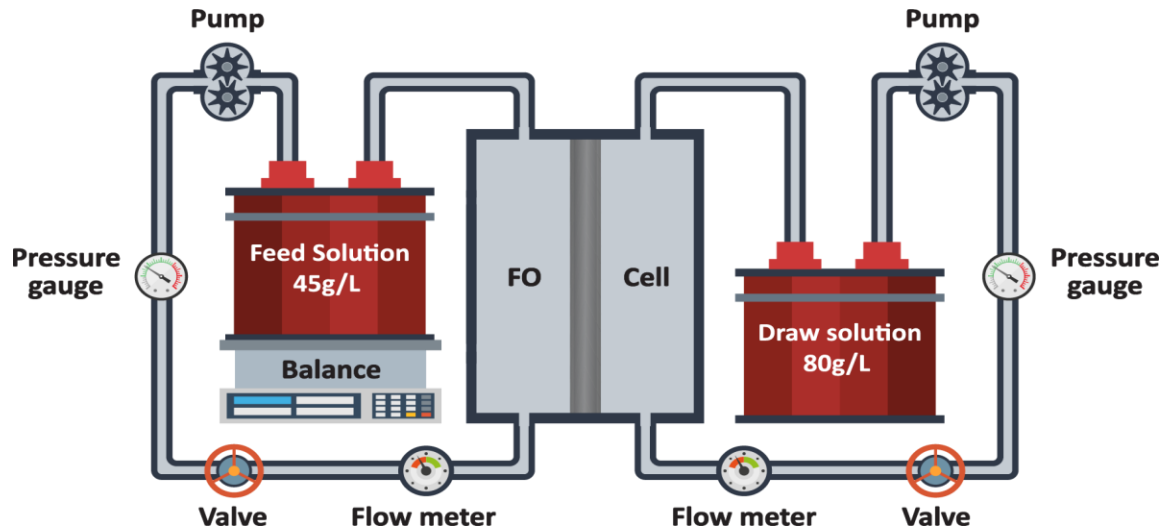
Figure 3: FO bench-scale unit configuration.

2.4 Experimental work

Each run of the FO process lasted for 5 hours, and each membrane was washed with DI water for 30 minutes at the end of the process, before using in the next run. For all FO processes, permeation flux collected in the first 10 minutes was discarded until the membrane filtration process is stabilized. The first set of FO tests was designed to calculate permeation flux at hydraulic pressure gradient equals to zero (ΔP=0) then a feed pressure in a range of 1 to 4 bar was applied in the PAFO process. Divalent ions, Ca^{2+}, Mg^{2+} and $SO4^{2-}$ concentrations were measured at the beginning and after each experiment.

Permeation flux in LMH was calculated after measuring the variation of the weight of the FS during the process according to the following equation (Zhang et al., 2014):

$$J_W = \frac{\Delta W}{A.\Delta t} \qquad (3)$$

ΔW is the difference in the weight of FS in kg, A represents the membrane area in m^2 and Δt is time interval in hours (h).

At the beginning and the end of each FO run, the concentrations of Ca^{2+} and Mg^{2+} in the DS was measured using an ion chromatography machine 7900 ICP-MS provided by Agilent technologies. The concentrations of $SO4^{2-}$ were measured using Dionex VWDIC manufactured by HPIC. These three ions were the only ions studied and measured in this study as they are accountable for the non-alkaline scale development in the MSF plants in the

form of Mg$SO_4$and CaSO_4 (Tang et al., 2010). Reducing the concentration of these ions in the DS using the FO process will help in controlling scale formation and depositions, using a diluted feed solution in the MSF process (Hawari et al., 2016).

3. Results and Discussions

3.1 Impact of membrane materials and orientations

3.1.1 Permeation flux

The impact of applying hydraulic pressures on the FS side was investigated in terms of permeation flux. The first set of experiments measured permeation flux at feed pressure between 0 and 4 bar for 5 hours in the AL-FS mode, and both membranes (TFC & CTA) were tested for this orientation. In the PAFO experiments, a feed pressure between 1 and 4 bar with 1 bar interval was applied to the FS. The temperature of the DS and the FS was 40°C and 25°C, respectively, which represent the temperature of the brine reject from the MSF plant and the seawater in the Middle East (Thabit et al., 2019). **Figure 4A and 5A** present the variation in the permeation flux throughout 5 hours tests at different applied pressures on the FS in the AL-FS mode for the TFC and the CTA membranes. Results show that permeation flux at 0 bar was around 7.4 LMH compared to 14.8 LMH at 4 bar for the TFC FO membrane and 6.4 LMH and 8 LMH at 0 and 4 bar respectively, for the CTA FO membrane. Indeed, increasing the feed pressure from 0 to 4 bar resulted in a 50% more permeation flux in the TFC membrane and 25% more permeation flux in the CTA membrane. The thicker support layer of CTA membrane led to an intense internal concentration polarization, which reduced permeation flux compared to the TFC membrane that has 50% thinner support layer (**Table 1**). Generally, results show a drop in the permeation flux over time because of the concentration of the FS and the dilution of the FS, which caused a sharp drop in the osmotic driving force and therefore lowered the permeation flux (Thabit et al., 2019). There is a remarkable decline in permeation flux over time, particularly in the PAFO test performed with a TFC membrane. The decline in the permeation flux when using TFC was quick in the first 30 minutes and became steady to the end of the experiments. The drop in the permeation flux in the CTA membrane was gradual throughout the 5 hours tests. For example, there was 22.6% and 19.9% reduction in the permeation flux in the FO tests with TFC and CTA

membranes, respectively. Indeed, there was 65% and 27% decrease in the permeation flux in the PAFO tests at 4 bar feed pressure with the TFC and CTA membranes, respectively. This decrease in permeation flux is probably due to the higher permeation flux in the TFC membrane that caused a sharp fall in the osmotic driving force in the PAFO tests.

The TFC membrane from Porifera achieved higher permeation flux in the FO and PAFO tests in comparison with the CTA membrane, knowing that higher permeation flux was recorded in the PAFO tests. The results suggest that higher dilution of the brine reject (the draw solution) would be accomplished in the PAFO test using Porifera TFC membrane in the AL-FS orientation.
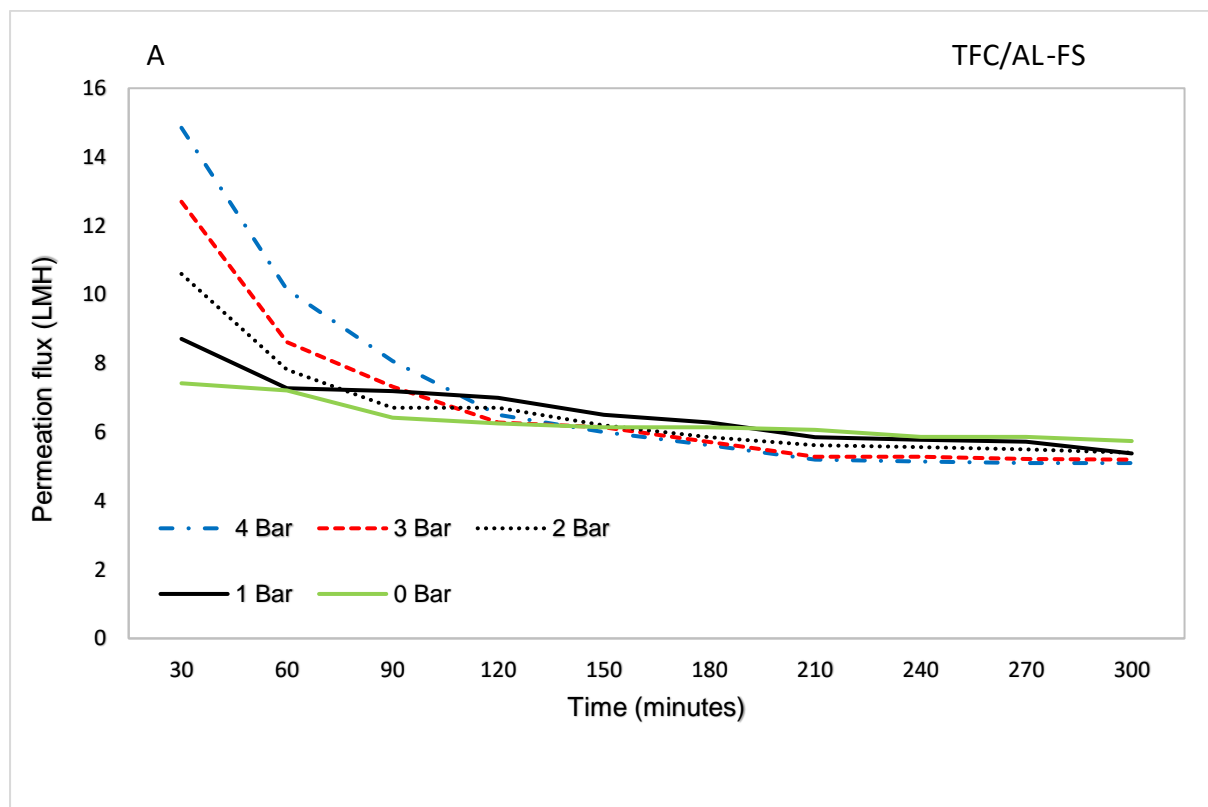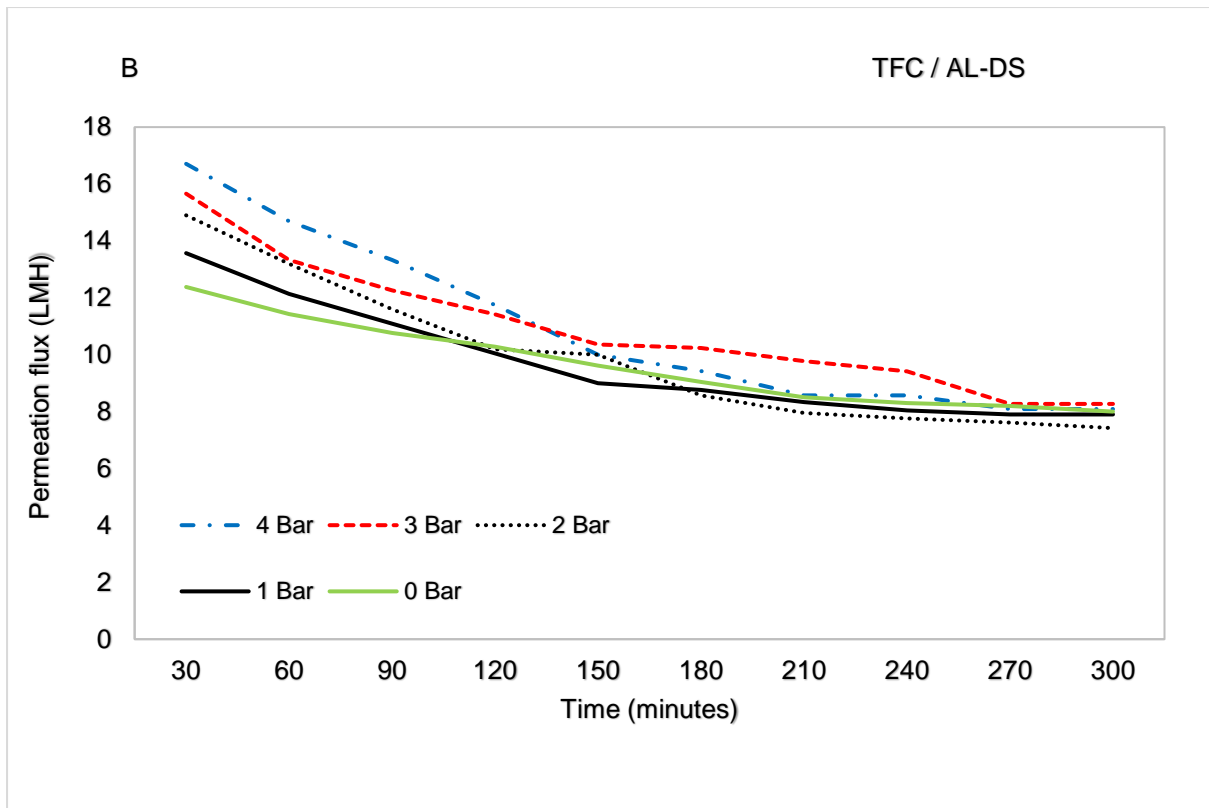
Figure 4: Permeation flux overtime at hydraulic pressures between 0 and 4 bar in theTFC membrane, (A) AL-FS mode and (B) AL-DS mode.
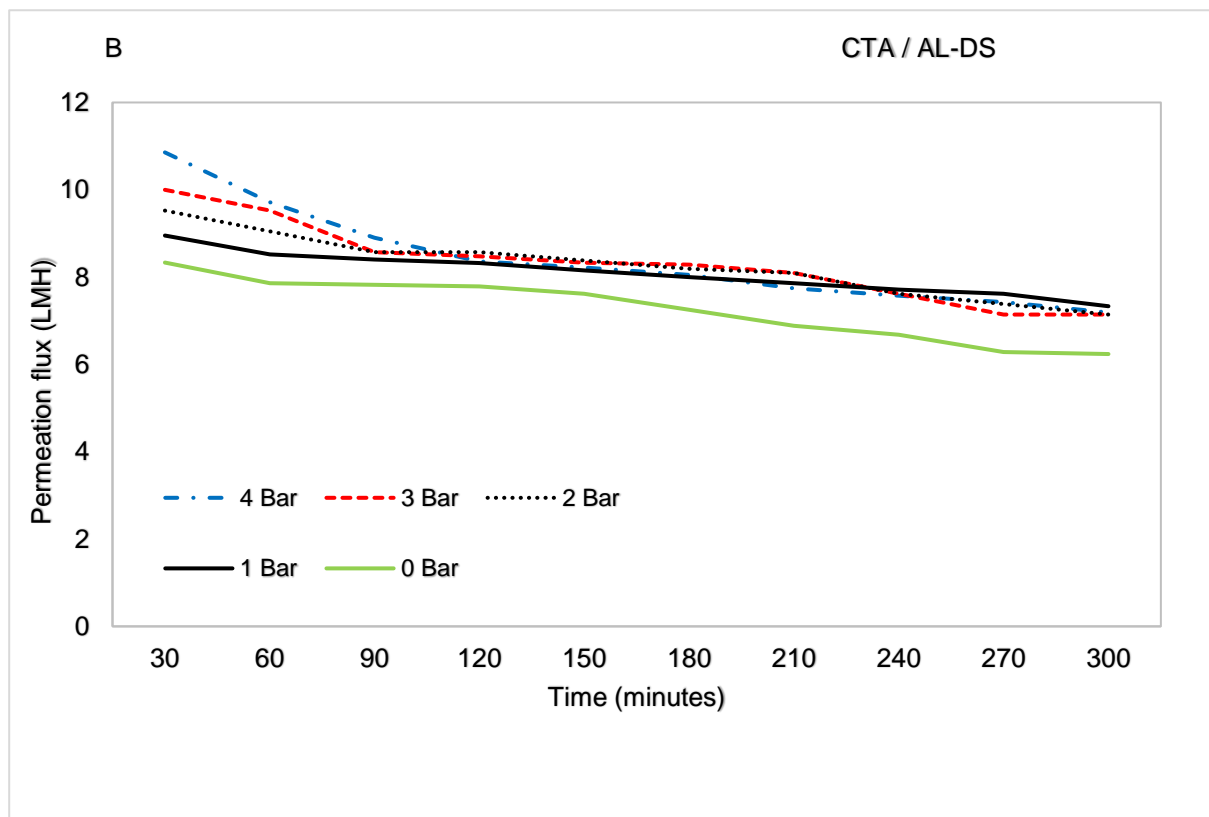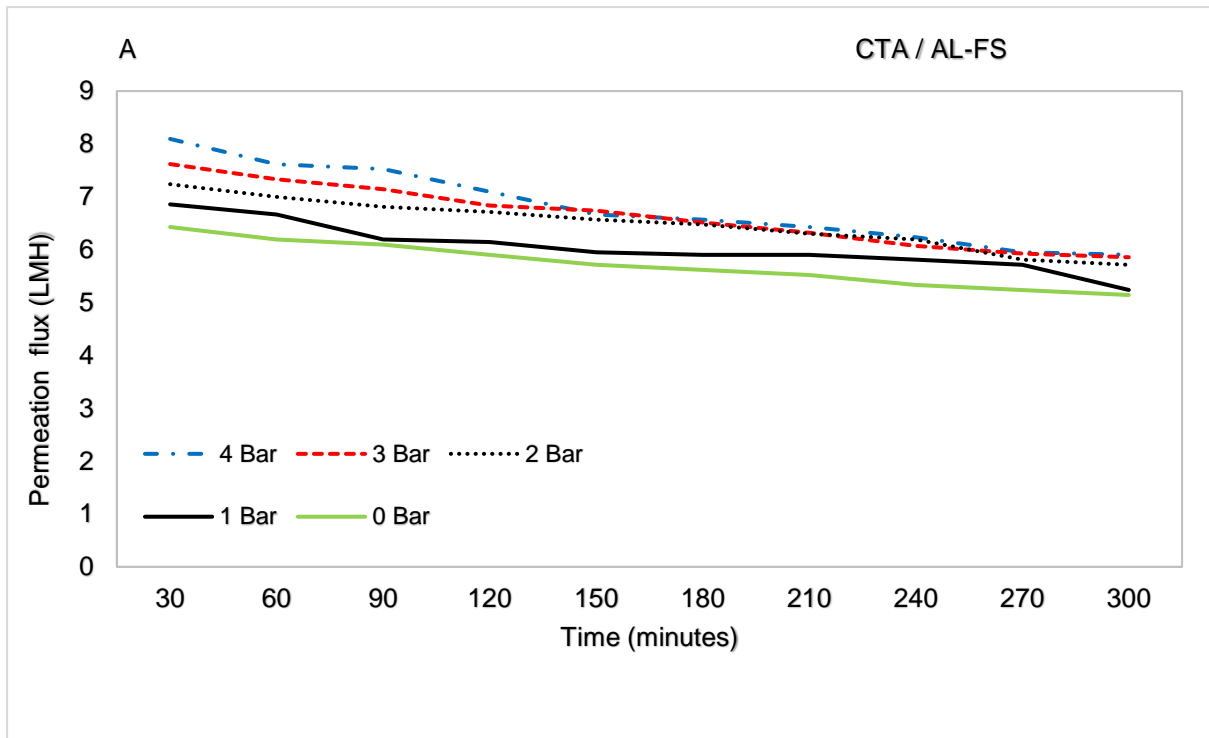
Figure 5: Change of permeation flux with time at different applied pressures using CTA membrane, (A) AL-FS and (B) AL-DS.

In the next set of experiments and under the same conditions, both types of membranes were tested with AL facing the DS and results are presented in **Figures 4B and 5B**. These two figures

illustrated the profile of permeation flux in the FO and PAFO tests when the AL-DS mode was applied using TFC and CTA membranes. What is noticeable on a large scale is that a greater permeation flux was achieved in all experiments tested in the AL-DS mode in comparison with the AL-FS operating mode. According to **Figures 4A and 4B**, permeation flux in the TFC membrane tested in the AL-FS at 0 bar feed pressure was 7.4 LMH. In contrast, permeation flux was 12.4 LMH in the membrane tested in the AL-DS. Permeation flux increased by 67% by altering the membrane mode from the AL-FS to the AL-DS, indicating that more permeation flux and dilution of the brine reject DS was achieved. For the PAFO process at 4 bar feed pressure using TFC membrane, permeation flux in the Al-FS direction was 14.9 LMH while it was 16.7 LMH in the PRO mode, recording more than 12% increase in the permeation flux after changing the membrane orientation. For the CTA membrane at 0 bar, there was 29% increase in permeation flux by altering the orientation of the membrane from the AL-FS to the AL-DS mode (**Figures 5A and 5B**). In contrast, there was 34% more permeation flux in the CTA membrane operating at 4 bar due to altering the orientation from the AL-FS to the AL-DS mode (**Figures 5A and 5B**). The results are compatible with previous studies in which FO membrane operating in the PRO mode exhibited greater permeation flux; there was an agreement in these studies that concentration polarization is lower and more controllable in the AL-DS mode (Hawari et al., 2018; Hawari et al., 2016; Mazlan et al., 2016; Tang et al., 2010; Xu et al., 2010).

Furthermore, permeation flux was higher in all the experiments using TFC membrane compared to the permeation flux when CTA membranes were used. For example, TFC membrane tested in the AL-FS at 0 bar exhibited 83% more permeation flux in comparison with the CTA membrane tested in the AL-FS direction. Results also showed that at 4 bar feed pressure, the permeation flux in the TFC membrane tested in the AL-DS direction was 54% more than that in the CTA membrane tested under the same operating conditions. The reason for this is ascribed to the hydrophilicity of the TFC membrane and its thinner support layer (**table 1**), which led to a higher permeation flux in the TFC membrane. The other reason for higher permeation flux in the TFC membrane in AL-DS is probably due to the higher hydrophilicity of its support layer that promoted the permeation and diffusion of the FS to the DS (**Figure 2**).

Figure 6 presents the calculated average permeation flux at 0 to 4 bar feed pressure for both TFC and CTA membranes and in the AL-FS and AL-DS directions. For the TFC membrane,

results show that a maximum average permeation flux of 9.57 LMH was achieved at 4 bar hydraulic pressure in the AL-DS direction. Under the same operating conditions, the maximum reported average permeation flux of the CTA membrane was 8.4 LMH, this 12% less than the average permeation flux achieved in the TFC membrane. For the TFC and CTA membrane operating at 4 bar in the AL-FS orientation, there was 8.6% difference in the average permeation flux in favour of the TFC membrane. Comparing to the AL-DS mode, the difference in the average permeation flux between the TFC and CTA membrane working the AL-FS mode was lower. And this caused by the complexity of the ICP phenomenon, which affected the driving force across the membrane despite the thinner structural parameter of the TFC membrane.

In general, permeation flux declined more rapidly in the PAFO process due to the greater permeation flux, which caused a steep decline in the osmotic pressure. Practically, a faster decline in the osmotic driving force requires fewer FO modules and this will reduce the capital cost for seawater pretreatment by the FO process.
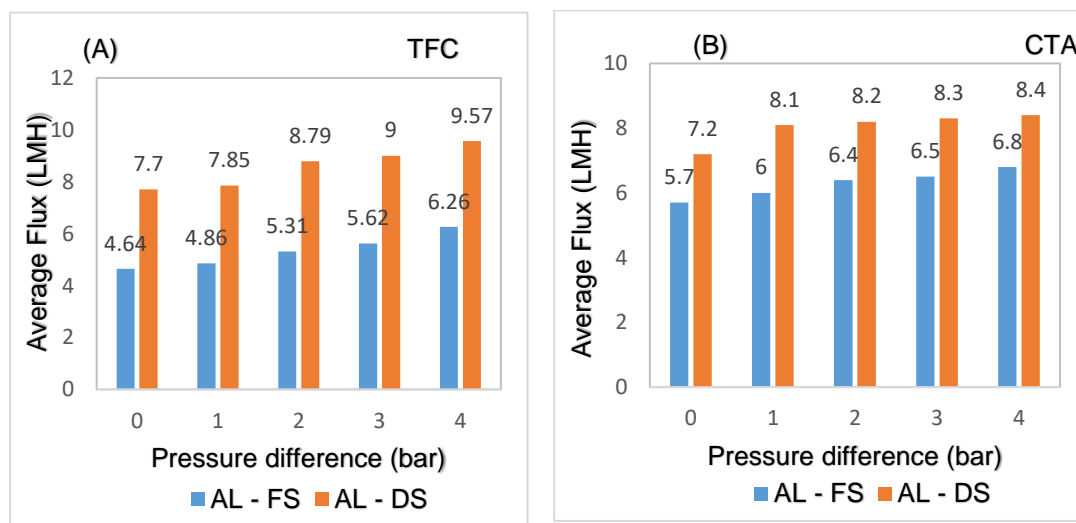

Figure 6: The average membrane flux at different applied pressures using (A) TFC membrane and (B) CTA membrane in both orientations, (AL-FS) and (AL-DS).

3.1.2 Flux reduction

Each used membrane was washed for 30 minutes with a DI water at the end of the first test and reused in another run. Then, permeation flux was estimated at the end of the second test to investigate the reduction in the permeation flux due to irreversible fouling of the

membrane. Losses in the permeation flux before and after cleaning with a DI water is attributed to the membrane fouling that cannot be removed by simple cleaning with DI water. It is worth mentioning that the DS and FS were not pre-treated before the FO process, and hence fouling would happen on the active and support layer of the membrane. **Table 2** shows that the turbidity of the DS and the FS are 2.43 and 1.47 NTU, respectively. It is expected that the fouling layer on the FS side might be denser due to the build-up of foulants on the membrane surface by the convective flow. In contrast, permeation flow from towards the DS side will remove loosely attached fouling materials away from the surface, in a mechanism similar to that in a backwash cleaning.

Figures 7A and 7B show the reduction of permeation flux in the FO experiment using TFC and CTA membranes, respectively. In the case of TFC membrane, the reduction in the permeation flux in the FO mode was 5.2% at 0 bar feed pressure and increased to 6.9% at 4 bar feed pressure (**figure 7A**). For TFC membrane operating in the PRO mode, the reduction in the permeation flux was 14.6 % in the PAFO test at 4 bar feed pressure and 10.4 % in the FO test. Apparently, FO tests performed in the PRO mode experienced a higher reduction in the permeation flux, and that was due to the poor mixing inside the support layer, reducing the effectiveness of the cleaning process. It is also observed the decline of the permeation flux in the PAFO tests was more severe at elevated feed pressures as a result of the dense and compacted fouling layer inside the support layer (SL).

Similarly, for the CTA membrane, **Figure 7B** shows that permeation flux reduction was greater at 4 bar feed pressure. In contrast, the TFC membrane exhibited a greater reduction in the permeation flux in comparison with the CTA membrane (**Figure 7B**). The highest recorded permeation flux reduction was 5.9% in the FO mode operating at 4 bar feed pressure; this is about 15% less than the reduction in the permeation flux in the TFC membrane tested under the same working conditions. The decline in the permeation flux in the CTA working in the AL-DS direction was three times less than that recorded in the TFC membrane under the same operating conditions. On the contrary, CTA membrane demonstrated a lower decline in the permeation flux when it was tested in the AL-DS direction. For example, the reduction in the permeation flux at 0 bar feed pressure was 3.2% in the AL-DS direction and 4.2% in the AL-FS direction. The corresponding results at 4 bar feed pressure were 5% in the AL-DS direction and 5.9% in the AL-FS direction. The reason for a lower permeation flux reduction in the CTA membrane when the FS was opposite to the SL and experiments with the DS opposite to the

SL is attributed to the combined effects of permeation flux in the membrane and the turbidity of FS and DS. The fouling layer was probably denser and compacted when the DS was against the SL due to the accumulation of the fouling materials from the high turbidity DS (2.43 NTU) in the porous SL. Unfortunately, low permeation flux in the CTA membrane aggravates the problem since fouling materials would not be flashed away from the membrane surface by the permeation flow, especially in the AL-FS mode. For this reason, cleaning with DI water was not effective for removing the fouling layer accumulated inside the dense SL of the membrane operating in the AL-FS direction. Accordingly, the CTA membrane performed better in the AL-DS direction due to the greater permeation flux (**Figure 5B**) while maintaining a lower reduction in the permeation flux. On the contrary, FO mode is the desirable working mode of the TFC membrane because of the high efficiency of the cleaning method in maintaining a low permeation flux reduction. For TFC membrane, permeation flux in the AL-FS mode at 4 bar feed pressure is almost twice that in the CTA membrane under same operating conditions.
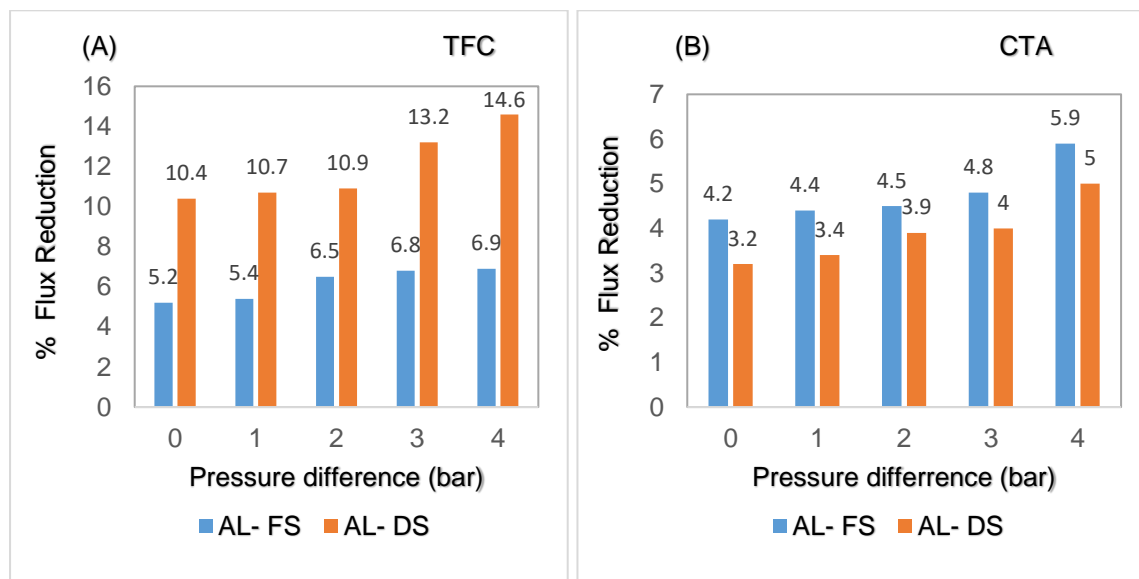

Figure 7: Flux Reduction in the membranes at different applied pressures, (A) TFC membrane and (B) CTA membrane.

Scanning electron microscope (SEM) images (**Figure 8**) reveals that the CTA membrane is more responsive to cleaning by DI water than the TFC membrane. A notable change in the morphology of the active and the support layer of used and washed Porifera TFC and FTSH$_2$O CTA membranes. For TFC membrane, cleaning with DI water achieved partial removal of

fouling materials from the membrane active while it was less successful in the removal of fouling layer on the support layer side. Ineffective cleaning with DI water of the TFC membrane explains the high reduction of permeation flux after cleaning. In contrast, cleaning with DI water was more effective in washing the fouling layer off the surface of the CTA membrane. The latter showed little fouling materials left on the washed active layer, and fouling materials became sparse after washing. These results explain the lower reduction in the permeation flux of the CTA membrane obtained after washing.
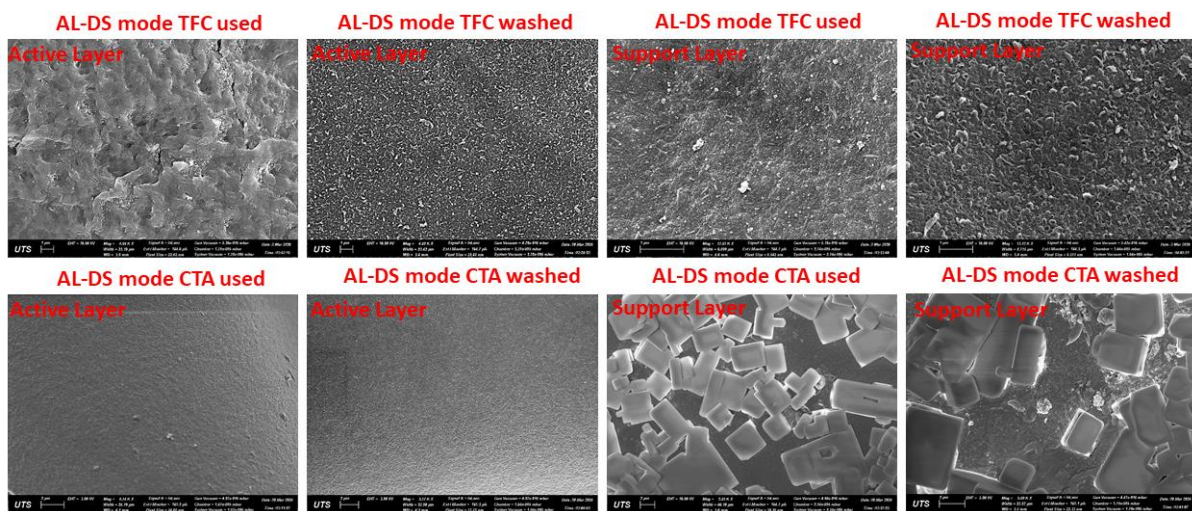

Figure 8: SEM images of membranes' active and support layer of used and washed TFC and CTA membrane. Images show fouling layer in the active and support layer of TFC and CTA at 2 bar hydraulic pressure.

3.1.3   Recovery rate

The recovery rate is estimated as the ratio of permeate flow to the feed flow according to the following expression:

$$Re = \frac{Q_p}{Q_f} 100\% \qquad (4)$$

Where, Q_p and Q_f are the flow rate of permeate and FS (L/min), respectively. Results, in general, shows that water recovery rate was higher in the AL-DS direction due to the greater permeation flux. **Figure 9** also reveals that the recovery rate in the FO process was greater at 4 bar feed pressure. TFC membrane achieved higher recovery rates than the CTA membrane due to higher membrane permeability and thinner structure parameter, which lessened the impact of concentration polarization inside the support layer (**Table 1**). The TFC membrane

achieved the highest recovery rate of 11.48% at 4 bar feed pressure in the AL-DS direction (**Figure 9A**). As for the CTA membrane, the highest recovery rate was 10.05% in the PRO mode at 4 bar (**Figure 9B**). Changing the orientation of the membrane from the AL-FS to the AL-DS direction, leading to more than 50% increase in the recovery rate. The increase in the recovery rate could be attributed to the greater permeation flux and low internal concentration polarization (ICP). When it is compared with the CTA membrane, TFC membrane achieved greater permeation flux and recovery rate at 4 bar feed pressure. The desirable operating mode for the TFC membrane is the AL- FS direction since such membrane orientation assures lower permeation flux reduction after cleaning with a DI water only (**Figure 7A**). For the TFC membrane, results in **Figure 7A** shows that 93.1% of the permeation flux was recovered in the FO test at 4 bar while 94.8% of the permeation flux was recovered in the FO tests at 0 bar. However, the latter operating conditions resulted in ~66% lower permeation flux in comparison with the FO process at 4 bar. Therefore, the FO process performed better in the AL-FS mode at 4 bar feed pressure using TFC membranes.
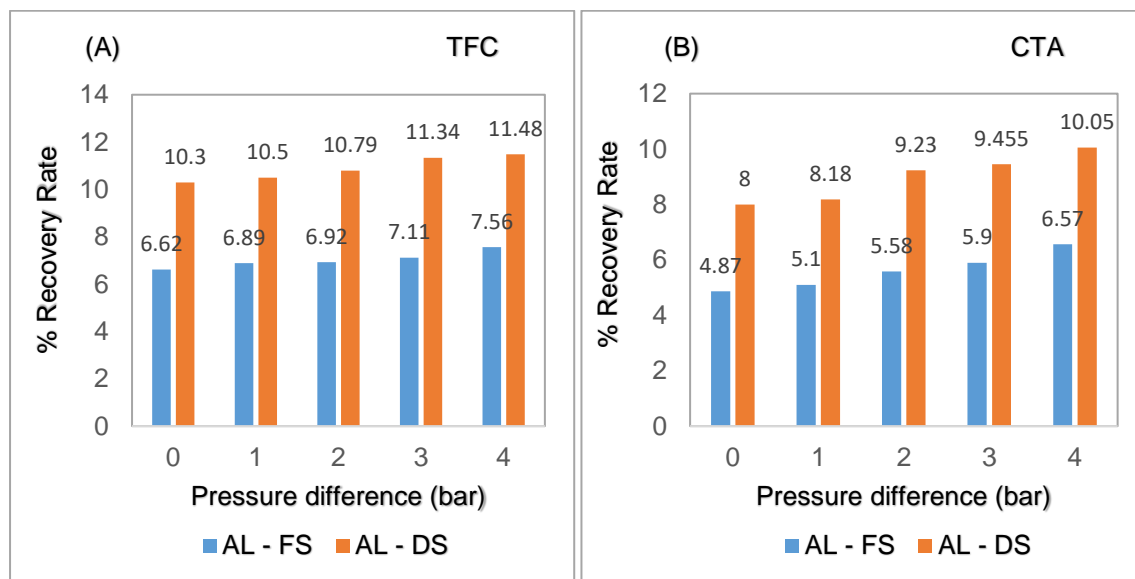

Figure 9: Recovery rate (%) at different applied pressures, (A) using TFC membrane and (B) using CTA membrane.

3.2 The concentration of Divalent Ions

It is discussed in the literature that the decrease in the concentration of the scale causing divalent ions will minimize the formation and deposition of non-alkaline scale on the surface of heat exchangers (Hawari et al., 2016). It is important to mention that ions reduction is the

decrease in the concentration of divalent ions in the DS after the pretreatment in the FO process. As mentioned earlier, the concentration of Mg^{2+}, Ca^{2+} and $SO4^{2-}$ in the DS was measured before and after each FO tests to report the concentrations after the FO pretreatment. All concentrations were reported and the percentage of reduction is presented separately for each ion in the FO experiments (**Figure 10**).

At first sight, results reveal that applying ascending feed pressure led to an increasing permeation flux and dilution of the DS. Comparing to the FO process at 0 bar, up to a four-time higher dilution of the DS was achieved by increasing the feed pressure from 1 to 4 bar. For example, 6% dilution of Mg^{2+} was achieved by the TFC membrane at 0 bar but Mg^{2+} dilution increased to 23% at 4 bar, that is 4 times more than that at 0 bar. For Ca^{2+}, 7% and 24 % dilution was achieved at 0 and 4 bar respectively and for $SO4^{2-}$, 9% and 28% dilution was achieved at 0 and 4 bar respectively. There is also a slight increase in the dilution of ions when the membrane was operating in the AL-DS direction in comparison with the AL-FS direction due to the higher permeation flow (**Figure 10A**). Furthermore, the TFC membrane showed a more substantial decrease in the divalent ions due to the higher permeation flux and ions rejection rate. Moreover, it is noticeable that for $SO4^{2-}$, the reduction is the highest amongst all other divalent ions (**Figure 10**), and this was attributed to its high rejection by the TFC membrane. When the CTA membrane was operating in the AL-DS direction, the dilution of Mg^{2+} ion was 10% and 21% at 0 and 4 bar, respectively. The dilution of Ca^{2+} ion was 6% and 25% at 0 and 4 bar, respectively and it was 7% and 21% for SO_4^{2-} at 0 and 4 bar, respectively. According to the data gathered about ions reductions, it is important to mention that applying 4 bar in the TFC tests with AL-FS mode is promising in seawater pretreatment to the MSF plant due to the considerable decrease in the divalent ions and low permeation flux reduction (**Figure 7A**).
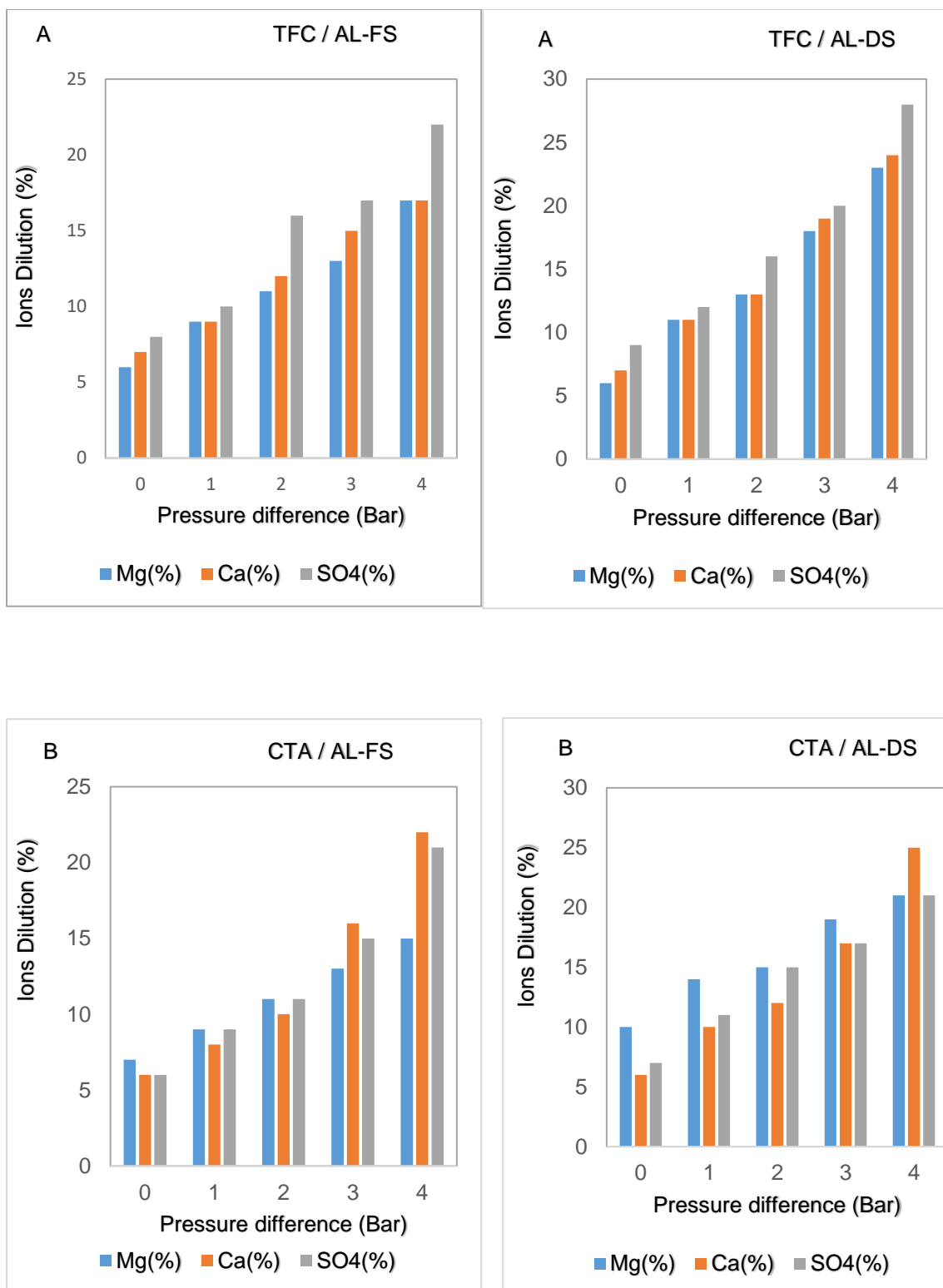
Figure 10: Ions dilution at different applied pressures, (A) TFC membrane and (B) CTA membrane.

3.3 Power consumption

Mathematically, specific power consumption (Es-kWh/m^3) can be estimated from the expression below:

$$E_S = \frac{P_f\,Q_f + P_D\,Q_D}{n\,Q_p} \qquad (5)$$

Where, P_f is the hydraulic pressure on the FS side (bar), P_D is the hydraulic pressure on DS side (bar), Q_f represents the FS flow rate (m^3/h), Q_D represents the DS flow rate (m^3/h), n represents the efficiency of the pump (0.8 in this study), and Q_p is the flow rate of permeate (m^3/h).

As shown in **Figure 11**, Es increased when the feed pressure was 4 bar. The results show that Es the in PAFO tests was higher than the Es in the FO tests. However, it is still low compared to the Es required for seawater desalination by the RO technology (McGovern, 2014). The highest specific power consumption was 0.1 kWh/m³ in the TFC membrane operating at 4 bar and in the FO mode. Results also show that the amount of power consumed in the AL-FS direction is slightly higher when it is compared with that of the AL-DS direction. For example, the Es in the CTA membrane at 4 bar was 0.08 in the AL-FS direction and 0.1 kWh/m^3 in the AL-DS direction (**Figure 11B**). The corresponding values in the TFC membrane at 4 bar, were 0.053 in the AL-FS mode and 0.065 kWh/m^3 in the AL-Ds direction (**Figure 11A**). According to equation 3, the lower permeation flow in the AL-FS direction in comparison with the AL-DS direction caused a slight increase in power consumption. Results in Figure 10 show that the highest Es in the FO pretreatment process is 0.1 kWh/m^3 whereas it is close to 2.5 kWh/m^3 in the RO technology for seawater desalination (McGovern, 2014). For the desirable operating condition with TFC membrane in the FO mode and at 4 bar, the specific power consumption was 0.065 kWh/m^3; this low power consumption underlines the great potential for applying the FO technology as a pretreatment process of seawater to the thermal MSF plant.
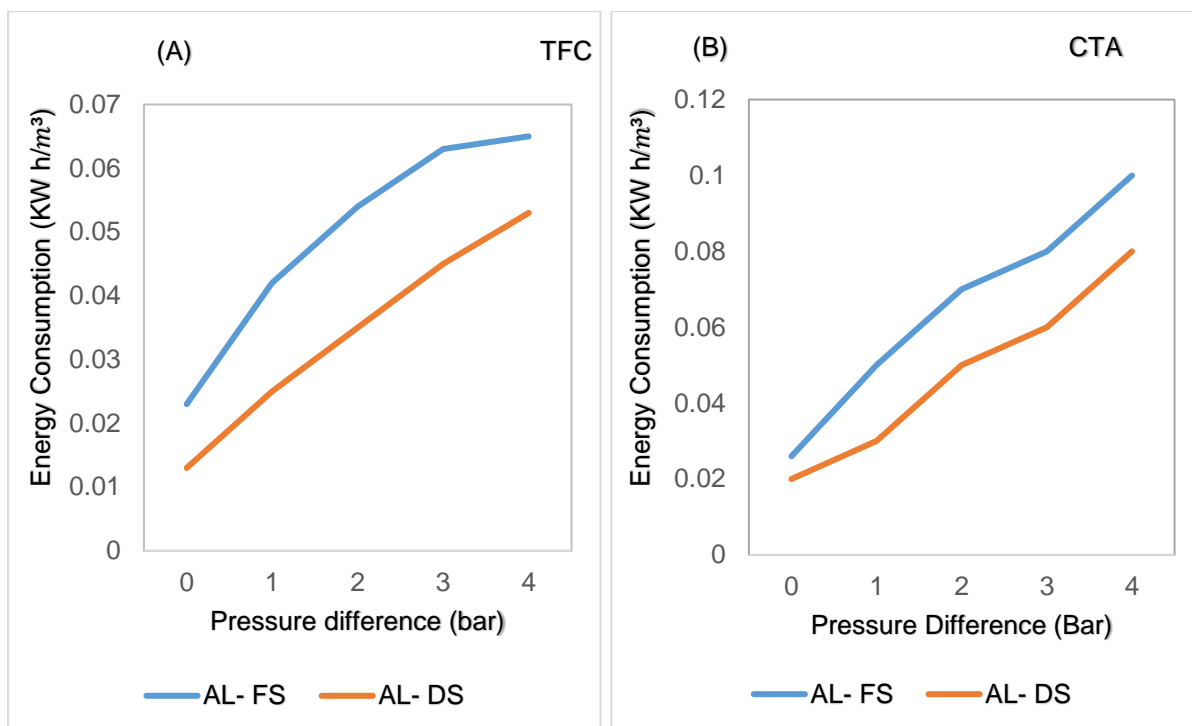
Figure 11: Energy consumption at different applied pressures, (A) using TFC membrane and (B) using CTA membrane.

4. Conclusions

FO and PAFO processes were tested for the pretreatment of seawater using commercial TFC and CTA membranes. The results showed that applying a small hydraulic pressure of the FS side led to an increase in the permeation flux. The permeation flux increased from 7.4 to 14.9 L/m²h by increasing the feed pressure up to 4 bar in the PAFO process with TFC membrane in the FO mode and at 4 bar. This significant improvement in permeation flux was achieved at a relatively trivial specific power consumption of 0.06 kWh/m³. CTA membrane, in general, demonstrated lower permeation flux than TFC at 4 bar pressure, 10.9 L/m²h, but the specific power consumption was slightly higher than that in the TFC membrane, 0.1 kWh/m³. Interestingly, the recovery of permeation flux in the fouled CTA after cleaning is higher than that in the TFC, and this was due to the characteristics of the fouling layer, which is loosely compacted due to the low permeation flux. Based on its low power consumption and high permeation flux, PAFO process at 4 bar using TFC membrane in the FO mode would be the preferable operating conditions. The latter operating condition has considerable permeation flux recovery of 93% after DI water cleaning. The results reveal the great potential and

feasibility of PAFO process for improving the performance of seawater pretreatment for MSF plant without compromising the advantage of low power consumption.

References

Al-Karaghouli, A. and Kazmerski, L.L. 2013. Energy consumption and water production cost of conventional and renewable-energy-powered desalination processes. Renewable and Sustainable Energy Reviews 24, 343-356.

Altaee, A., Mabrouk, A., Bourouni, K. and Palenzuela, P. 2014. Forward osmosis pretreatment of seawater to thermal desalination: high temperature FO-MSF/MED hybrid system. Desalination 339, 18-25.

Blandin, G., Verliefde, A.R., Tang, C.Y., Childress, A.E. and Le-Clech, P. 2013. Validation of assisted forward osmosis (AFO) process: Impact of hydraulic pressure. Journal of membrane science 447, 1-11.

Blandin, G., Vervoort, H., Le-Clech, P. and Verliefde, A.R. 2016. Fouling and cleaning of high permeability forward osmosis membranes. Journal of Water Process Engineering 9, 161-169.

Chung, T.-S., Zhang, S., Wang, K.Y., Su, J. and Ling, M.M. 2012. Forward osmosis processes: yesterday, today and tomorrow. Desalination 287, 78-81.

Coday, B.D., Heil, D.M., Xu, P. and Cath, T.Y. 2013. Effects of transmembrane hydraulic pressure on performance of forward osmosis membranes. Environmental science & technology 47(5), 2386-2393.

El Din, A.S., El-Dahshan, M. and Mohammed, R. 2002. Inhibition of the thermal decomposition of HCO_3^- A novel approach to the problem of alkaline scale formation in seawater desalination plants. Desalination 142(2), 151-159.

Gilron, J. 2014. Water-energy nexus: matching sources and uses. Clean Technologies and Environmental Policy 16(8), 1471-1479.

Hassan, A. 2006 Fully integrated NF-thermal seawater desalination process and equipment, Google Patents.

Hawari, A.H., Al-Qahoumi, A., Ltaief, A., Zaidi, S. and Altaee, A. 2018. Dilution of seawater using dewatered construction water in a hybrid forward osmosis system. Journal of Cleaner Production 195, 365-373.

Hawari, A.H., Kamal, N. and Altaee, A. 2016. Combined influence of temperature and flow rate of feeds on the performance of forward osmosis. Desalination 398, 98-105.

Intelligence, G.W., Yearbook, I.D., Summit, G.W. and Card, R. 2011. Global Water Intelligence. Global Water Intelligence 12(10), 1-72.

Jamil, S., Jeong, S. and Vigneswaran, S. 2016. Application of pressure assisted forward osmosis for water purification and reuse of reverse osmosis concentrate from a water reclamation plant. Separation and Purification Technology 171, 182-190.

Lyster, E., Kim, M.-m., Au, J. and Cohen, Y. 2010. A method for evaluating antiscalant retardation of crystal nucleation and growth on RO membranes. Journal of Membrane Science 364(1-2), 122-131.

Mabrouk, A.N.A. 2013. Technoeconomic analysis of once through long tube MSF process for high capacity desalination plants. Desalination 317, 84-94.

Madsen, H.T., Nissen, S.S., Muff, J. and Søgaard, E.G. 2017. Pressure retarded osmosis from hypersaline solutions: investigating commercial FO membranes at high pressures. Desalination 420, 183-190.

Mazlan, N.M., Marchetti, P., Maples, H., Gu, B., Karan, S., Bismarck, A. and Livingston, A.G. 2016. Organic fouling behaviour of structurally and chemically different forward osmosis membranes–a study of cellulose triacetate and thin film composite membranes. Journal of Membrane Science 520, 247-261.

McGovern, R.K. 2014. On the potential of forward osmosis to energetically outperform reverse osmosis desalination. Journal of Membrane Science 469, 245-250.

Oh, Y., Lee, S., Elimelech, M., Lee, S. and Hong, S. 2014. Effect of hydraulic pressure and membrane orientation on water flux and reverse solute flux in pressure assisted osmosis. Journal of membrane science 465, 159-166.

Tang, C.Y., She, Q., Lay, W.C., Wang, R. and Fane, A.G. 2010. Coupled effects of internal concentration polarization and fouling on flux behavior of forward osmosis membranes during humic acid filtration. Journal of membrane science 354(1-2), 123-133.

Thabit, M.S., Hawari, A.H., Ammar, M.H., Zaidi, S., Zaragoza, G. and Altaee, A. 2019. Evaluation of forward osmosis as a pretreatment process for multi stage flash seawater desalination. Desalination 461, 22-29.

Van der Bruggen, B. and Luis, P. 2015. Forward osmosis: understanding the hype. Reviews in Chemical Engineering 31(1), 1-12.

Xu, Y., Peng, X., Tang, C.Y., Fu, Q.S. and Nie, S. 2010. Effect of draw solution concentration and operating conditions on forward osmosis and pressure retarded osmosis performance in a spiral wound module. Journal of membrane science 348(1-2), 298-309.

Yadav, S., Saleem, H., Ibrar, I., Naji, O., Hawari, A.A., Alanezi, A.A., Zaidi, S.J., Altaee, A. and Zhou, J. 2020. Recent developments in forward osmosis membranes using carbon-based nanomaterials. Desalination 482, 114375.

Zhang, S., Wang, P., Fu, X. and Chung, T.-S. 2014. Sustainable water recovery from oily wastewater via forward osmosis-membrane distillation (FO-MD). water research 52, 112-121.